Supplementary Material

Low field depolarization of NV⁻ centers through dipole-dipole coupling

C. Pellet-Mary[1], M. Perdriat[1], G. Hétet[1]

Laboratoire De Physique de l'École Normale Supérieure,

École Normale Supérieure, PSL Research University,

CNRS, Sorbonne Université, Université Paris Cité ,
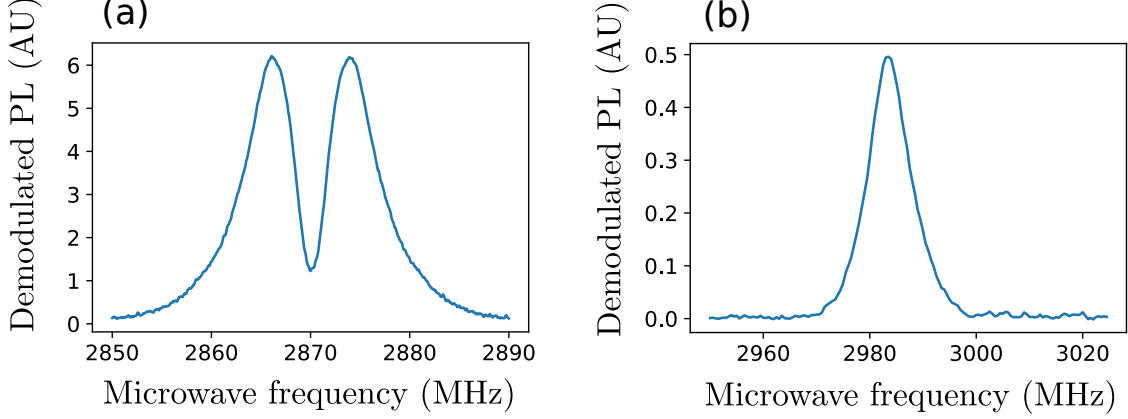
24 rue Lhomond, 75231 Paris Cedex 05, France.

CONTENTS

FIG. 1. ODMR measurement (a) in zero magnetic field, (b) in non-zero magnetic field when zooming on a single class transition

I.   NV⁻ GROUND STATE HAMILTONIAN IN LOW MAGNETIC FIELD

With zero external magnetic field, there are three possible sources of splitting of the $\{|+1\rangle, |-1\rangle\}$ manifold : local electric field, crystal strain and local magnetic field. Of these three causes, only the electric field can explain the shape of the ODMR line that we observe in zero external magnetic field (Fig. 1a) [4].

Indeed, random local magnetic field would produce a single broadened line while crystal strain would produce a shifting of the zero field splitting (ZFS) of the same order as the splitting of the levels, which would also blur the two transitions into a single line. On the other hand, due to the large difference between the longitudinal and transverse electric field susceptibilities ($d_\parallel = 0.35$ Hz cm/V and $d_\perp = 17$ Hz cm/V [5]), random local electric field will, on average, cause a splitting much stronger than its ZFS shifting and result in a two peak spectrum.

In our low magnetic field dipole-dipole coupling model, we will therefore neglect the contribution of the strain, local magnetic field and longitudinal electric field. We also don't take into account the hyper-fine structure of the NV center due to the large inhomogeneous broadening of the transitions (Fig. 1b). We will then consider the following spin Hamiltonian for the NV⁻ ground state :

$$\mathcal{H}_s = DS_z^2 + \gamma_e \vec{B}_{\text{ext}} \cdot \vec{S} + d_\perp \left[E_x(S_y^2 - S_x^2) + E_y(S_xS_y + S_yS_x) \right] \tag{1}$$
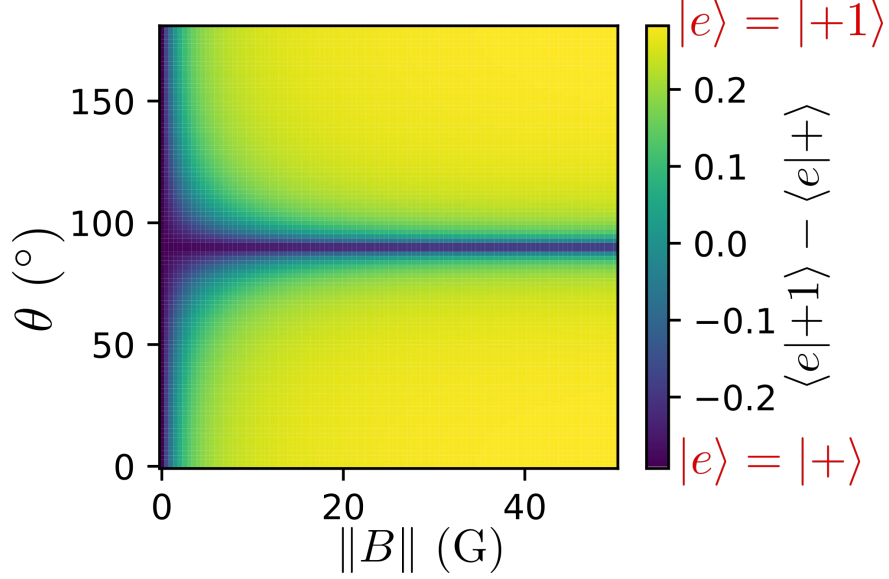
FIG. 2. Numerical simulations of the closeness of the Hamiltonian most excited state $|e\rangle$ with the states $|+1\rangle$ and $|+\rangle$, as a function of the magnetic field amplitude and angle θ with respect to the NV axis. A value of $d_\perp E_\perp = 4$ MHz was chosen

Where $D = 2.87$ GHz is the zero field splitting and $\gamma_e = 2.8$ MHz/G the gyromagnetic ratio of the electron.

In the absence of an external magnetic field, the symmetry in the (xy) plane allows us to chose the x direction along the electric field. The eigenstates of $\mathcal{H}_s$ then become $\{|0\rangle, |+\rangle = \frac{|+1\rangle + |-1\rangle}{\sqrt{2}}, |-\rangle = \frac{|+1\rangle - |-1\rangle}{\sqrt{2}}\}$.

In the presence of non-zero magnetic field, let us call the Hamiltonian eigenstates $\{|g\rangle, |d\rangle, |e\rangle\}$. Fig. 2 shows how close the $|e\rangle$ state is to the $|+1\rangle$ and $|+\rangle$ states as a function of the external magnetic field. Looking at the closeness of $|d\rangle$ to $|-1\rangle$ and $|-\rangle$ would show similar results, while $|g\rangle$ is pretty much equals to $|0\rangle$ for $B < 100$ G.

This tells us that in most cases, the $\{|0\rangle, |+\rangle, |-\rangle\}$ basis is only the good Hamiltonian basis for magnetic field smaller than a few Gauss, except in the case of pure transverse magnetic field where the $\{|0\rangle, |+\rangle, |-\rangle\}$ basis remains a good basis even for sizable magnetic fields.

II. SAMPLES

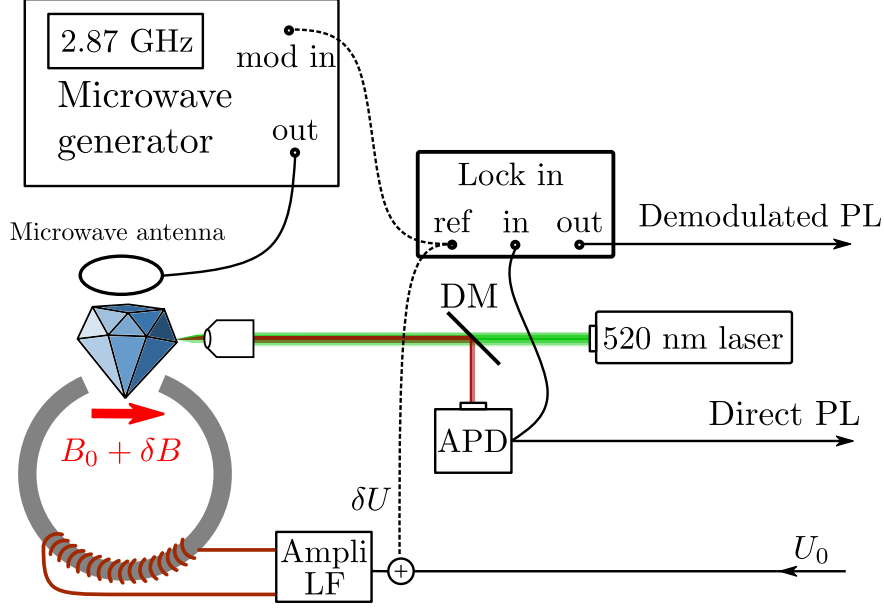A faire à la fin pour être sur des figures du main text.

FIG. 3. Experimental Setup

III.   EXPERIMENTAL SETUP

Fig. 3 shows the general purpose experimental setup used for all the experiments presented in this article.

The optical polarization and readout of the spins is done by focusing a green laser on the diamond sample with an objective lens([ref]), and collecting the back-scattered red fluorescence from the NV center on an avalanche photo-diode (APD, REF). The laser is filtered out using a dichroic mirror (DM, ref) and a notch filter. The NV^0 fluorescence is filtered using an additional 645 nm longpass filter.

The laser used here is a [REF], providing pulses of X ns at a rate of 20 MHz, with an average power of $0.5 \sim 5$ mW. The trigger of the pulses is generated externally in order to achieve fast gating of the laser for the T_1 measurement. We previously did similar experiment using a continuous 532 nm laser and observed no difference in the behavior of the spins.

The magnetic field is provided by a homemade electromagnet composed of a c-shape iron core and copper wires. The magnet is mounted on two mechanical rotation stages, allowing a control on the polar and azimuthal angle of the magnetic field within a fraction of a degree and is alimented through a low frequency amplifier (REF)

The microwave field is generated by a Rhode & Shwarz SMB 100A and is emitted with a handmade loop antenna. The field is gated by a [REF minicircuit] switch controlled

externally.

A lock-in amplifier is used either to modulate the microwave amplitude for ODMR measurement, or to add an oscillatory magnetic field for the magnetometry protocol. In both case we use a modulation frequency ~ 1 kHz and demodulate the APD signal.

IV. EXPERIMENTAL DETAILS

A. T_1 fitting Protocol

The T_1 profile that we observe with our samples is neither purely exponential, nor purely stretched exponential, which is to be expected when the dipole-dipole spin decay is comparable to the phonon decay.

Fig. 4 shows the result of a lifetime measurement, measured with the subtraction protocol described in the main text, for zero and non-zero magnetic field. The result is fitted with exponential and stretched-exponential (with a stretch factor $\beta = 0.5$) functions. We can see that for the shorter lifetime (zero field), the measurement follows more closely the stretched-exponential profile, while the longer lifetime is closer to the exponential one (except at very short times).

In order to directly compare the results from different magnetic fields, we therefore decided to fit each T_1 measurement with both a stretched and exponential decay : $S(\tau) = A \exp\left(-\frac{\tau}{T_1^{\mathrm{ph}}} - \sqrt{\frac{\tau}{T_1^{\mathrm{dd}}}}\right)$. To add consistency to the measurement of T_1^{dd}, we decided to fix T_1^{ph} for each sample, leaving T_1^{dd} and the signal amplitude as the only free parameters in the fitting procedure. The value chosen for samples [REF] and [REF] was $T_1^{\mathrm{ph}} = 3.62$ ms. Fig. 1 of the main text shows the result of fitting the same two measurement with this formula.

An other possibility would be to use an arbitrary stretched factor in the fitting function : $S(\tau) = A \exp\left(-(\frac{\tau}{T_1^{\mathrm{ph}}})^\beta\right)$. Fig. 5 shows the optimal β parameter as a function of the external magnetic field, which confirms that the T_1 profile gets closer to a pure stretched-exponential in zero magnetic field.
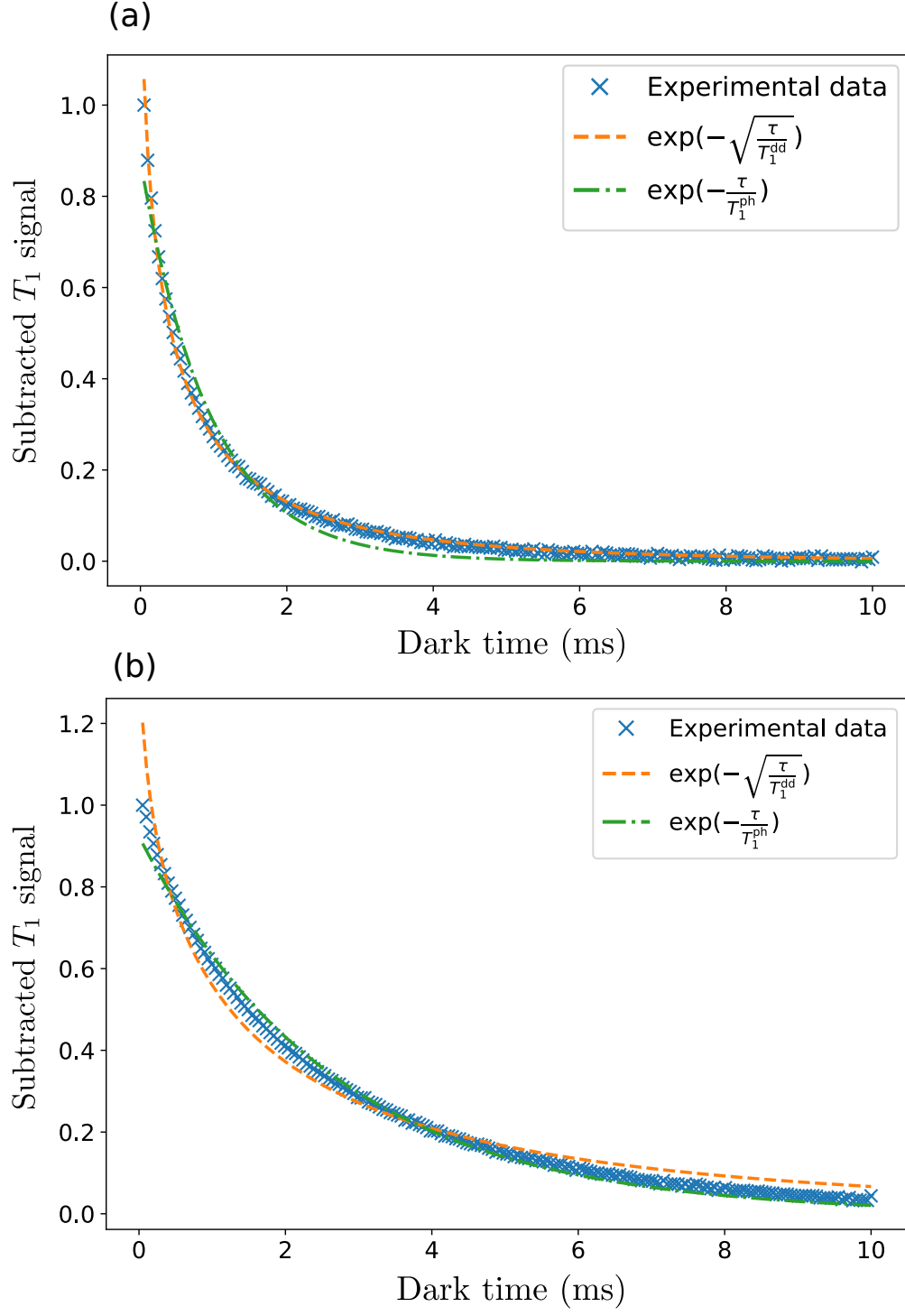
6

FIG. 4. T_1 measurement with purely exponential and purely stretched exponential fits (a) in zero magnetic field (b) in non-zero magnetic field
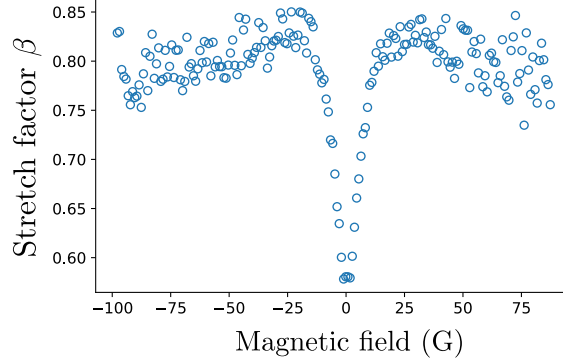
FIG. 5. Best stretch factor β for a T_1 fit of the form $f(\tau) = A\exp\left(-(\frac{\tau}{T_1})^\beta\right)$ as a function of a randomly oriented magnetic field amplitude

B.   Spectral range of the dipole-dipole cross-relaxations

An experimental signature of the fluctuator hypothesis developed in [2] is to measure the depolarization rate for two near-resonant classes : if there are indeed very fast decaying NV centers (fluctuators with lifetime $T_1^f < 100ns$), then the spectral width of the fluctuator would be increased beyond $1/T_2^*$ (which we assume to be homogeneous among all spins in the crystal), which means that they would be able to exchange spin quanta (flip-flop) with non-resonant NV detuned by $\Delta\nu$ such that $2\pi/T_1^f > \Delta\nu > 2\pi/T_2^*$

In order to verify this claim, we have to measure the spectral overlap between two classes, which in the absence of fluctuator should be proportional to the flip-flop rate, and compare it to the actual flip-flop rate which we can measure through the depolarization rate of the spins.

Fig. 6 shows the results of such an experiment where we measured the stretched part of the NV's decay rate, which is very well fitted by a Lorentzian of width $\sigma = 8.04MHz$, and compare it to an ODMR line of a single class of NV centers, stretched by a factor of $\sqrt{2}$ and 2 to simulate the spectral overlap of the two classes (discussed bellow). One should notice that, not only is $1/T_1^{\rm dd}$ significantly larger than the ODMR profile, it also doesn't have the same shape.

We should note that this broadening can not be explained by the dipole-dipole interaction strength : for a sample with 3 ppm of NV centers, the average dipole-dipole interaction strength between two nearest NV centers $J_0/r^3 \sim 27$ kHz which is several order of magnitude lower than the broadening we observe.
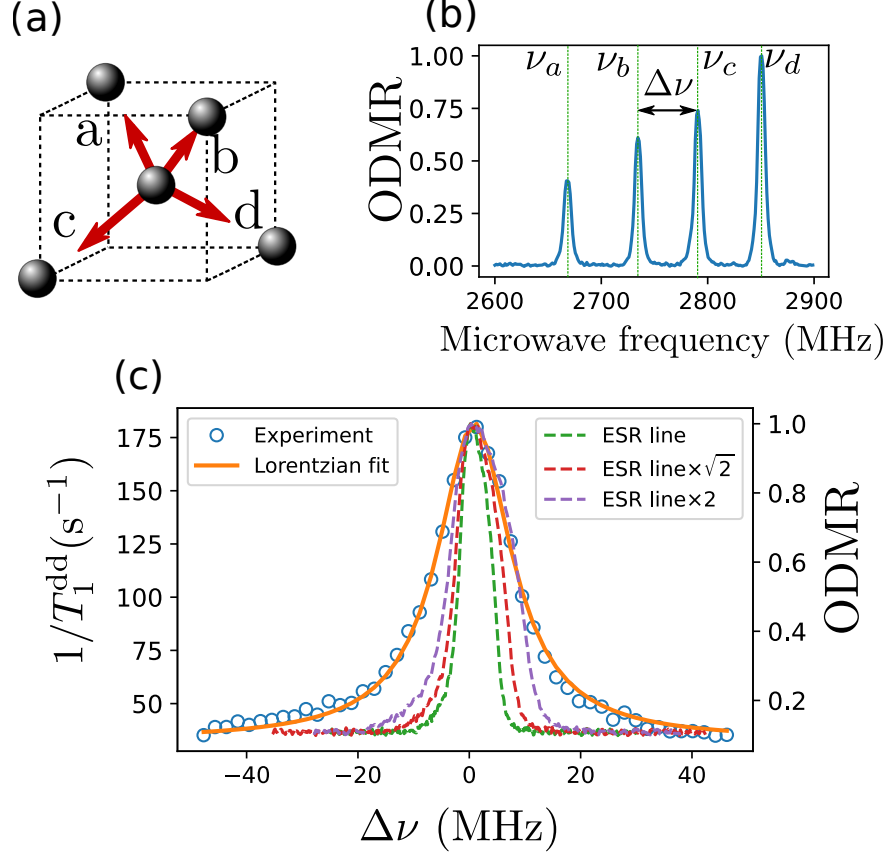
FIG. 6. Dipole-dipole depolarization for two near-resonant classes. (a) Sketch of the four possible orientations ("classes") in a single crystal diamond lattice. (b) ODMR spectrum showing four $|0\rangle \rightarrow |-1\rangle$ resonances corresponding to the four spin classes. The detuning $\Delta\nu$ between the classes b and c was controlled by changing the orientation of the external magnetic field.(c) Stretch part of the lifetime decay for the spins resonant with ν_c as a function of the detuning $\Delta\nu$ (blue circles), fitted by a Lorentzian with half width at half maximum 8.04 MHz. Single class ESR line stretched by a factor of $1, \sqrt{2}$ and 2 are added for comparison

As illustrated on Fig. 7, we define the spectral overlap $S(\Delta\nu)$ between two spins of spectral response $S_1(\nu)$ and $S_2(\nu)$, centered respectively on the frequencies ν_1 and ν_2 where $\Delta\nu = \nu_2 - \nu_1$ as :

$$S(\Delta\nu) = \int S_1(\nu, \nu_1) S_2(\nu, \nu_2) d\nu \qquad (2)$$

In order to approximate the spectral overlap in our experiment, we will consider the analytical solution in the Gaussian and Lorentzian case :

- For two gaussians of standard deviation σ, the spectral overlap as a function of the
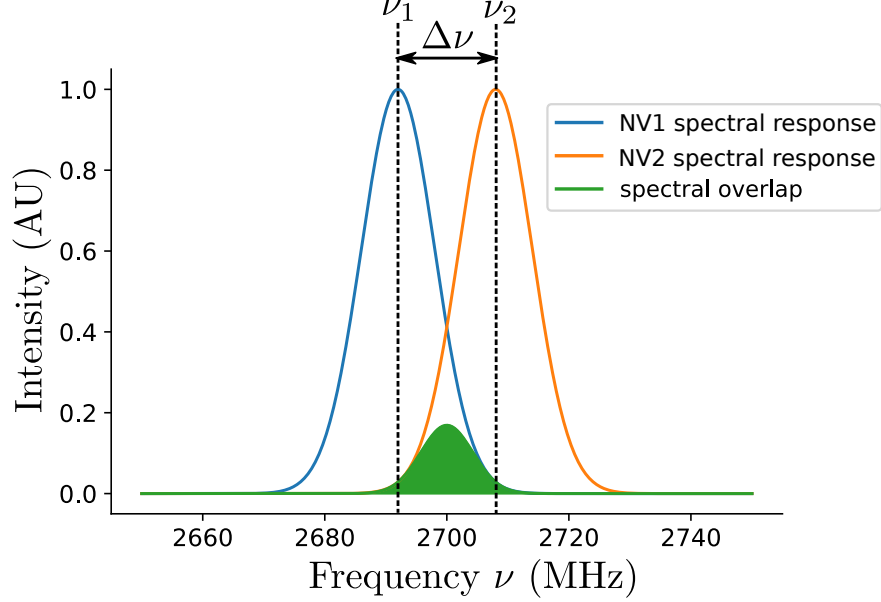
FIG. 7. Illustration of the spectral overlap for two gaussian spectra

detuning $\Delta\nu = \nu_1 - \nu_2$ is itself a gaussian of standard deviation $\sigma' = \sqrt{2}\sigma$. :

$$S(\Delta\nu) \propto \int \exp\left(-\frac{(\nu - \nu_1)^2}{2\sigma^2}\right) \exp\left(-\frac{(\nu - \nu_2)^2}{2\sigma^2}\right) d\nu$$

$$\propto \exp\left(-\frac{(\Delta\nu)^2}{4\sigma^2}\right)$$

- For two Lorentzian profile with width σ, the overlap function is itself a Lorentizan with width $\sigma' = 2\sigma$:

$$S(\Delta\nu) \propto \int \frac{1}{1 + \frac{(\nu - \nu_1)^2}{\sigma^2}} \cdot \frac{1}{1 + \frac{(\nu - \nu_2)^2}{\sigma^2}} d\nu$$

$$\propto \frac{1}{1 + \frac{(\Delta\nu)^2}{4\sigma^2}}$$

The ODMR lines that we measure are neither Lorentzian nor Gaussian (although they tend to be closer to Gaussians), and can even be asymmetric. Nevertheless, the overlap between two classes can most likely be approximated by a single class ODMR profile stretched by a factor between $\sqrt{2}$ and 2.

C. Effect of laser polarization

Previous studies [1, 3] reported the presence of a photoluminescence dip in zero magnetic field which was heavily dependent on the laser polarization angle with respect to the diamond
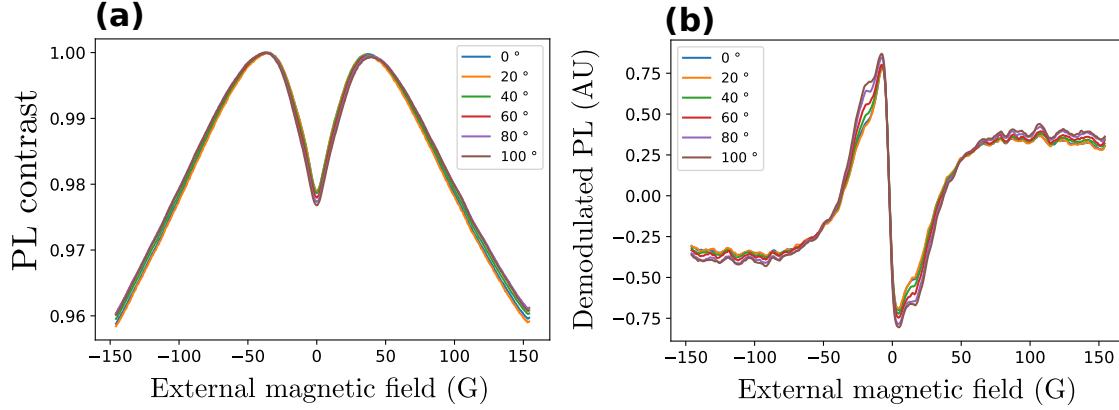
FIG. 8. Effect of the polarization of the incident laser. (a) Photoluminescence as a function of randomly oriented magnetic field amplitude for various polarization angle. (b) Demodulated PL in the same conditions

axes and the magnetic field.

We did not observe a strong dependence on the laser polarization with the samples used in this study. Fig.8 shows the photoluminescence from one of our sample as a function of the magnetic field, either directly or with a modulation of the magnetic field, for 6 randomly chosen polarization angle and saw no major difference.

In particular, we did not observe the apparition of an anti-line inside the main dip, unlike what was observed in the two previously cited work. We expect that the main reason behind the different behaviors is that we seem to observe far grater spin depolarization in zero-field, which we attribute to dipole-dipole coupling, and that this effect could hide smaller effects such as the one related to the laser polarization.

D. Alignment of B

La faudrait p-e montrer ce qu'il se passe pour un décalage de quelques degrés. A voir si j'ai déja les plots

V. EXTENSION OF THE FLUCTUATOR MODEL TO LOW MAGNETIC FIELDS

A. Summary of the NV-fluctuator model

As mentioned in the main text, we base our analysis on the NV-fluctuator model developed in [2] whose main hypothesis and conclusions we will summarize here :

The NV^- centers in the crystal are divided between two categories : "normal" NV centers (simply called NV) which, in the absence of dipole-dipole coupling would have a phonon-limited T_1 ($T_1^{NV} \sim$ ms), and fluctuators who are NV centers with an additional, fast, depolarization mechanism, such that their lifetime $T_1^f < 100$ ns. Having such a short lifetime, the fluctuators are almost unpolarized by the green laser, making them invisible in standard optical NV measurement protocol (T_1, ODMR, etc.).

Assuming a homogeneous distribution of the fluctuators in the bulk of the crystal, the authors of [2] conclude that the fluctuators create an additionnal decay channel for the NV population, through dipole-dipole interaction, characterized by a decay rate γ which follows the probability distribution :

$$\rho(\gamma) = \frac{e^{-1/(4\gamma T)}}{\sqrt{4\pi\gamma^3 T}} \tag{3}$$

Where the timescale T is defined as

$$\frac{1}{T} = \left(\frac{4\pi n_f J_0 \bar{\eta}}{3}\right)^2 \frac{\pi}{\gamma_f} \tag{4}$$

Where n_f is the fluctuator density in the crystal in nm^{-3}, $J_0 = 52$ MHz $\cdot$ nm^3 is the characteristic dipole-dipole strength between two spins, γ_f is the fluctuator intrinsic decay rate and $\bar{\eta}$ is a dimension-less number which characterizes the average dipole-dipole interaction between the NV centers and the fluctuators (resonance conditions, relative orientations etc. Further details are given below).

The polarization dynamics of the averaged ensemble of NV centers then follows :

$$P(t) = \int_0^\infty \rho(\gamma)\, e^{-\gamma t} d\gamma = e^{-\sqrt{t/T}} \tag{5}$$

Which corresponds to the stretched-exponential part of the lifetime measurement.

B. Dipole-Dipole Hamiltonian between two NV$^-$ centers

We consider a system composed of an NV center interacting dipolarly with a fluctuator.

$$\mathcal{H}_{\text{tot}} = \mathcal{H}_1 + \mathcal{H}_2 + \mathcal{H}_{\text{dd}} \tag{6}$$

Where $\mathcal{H}_1$ and $\mathcal{H}_2$ are the single particle Hamiltonian of the NV and fluctuator, described by the equation (1), and $\mathcal{H}_{\text{dd}}$ is the dipole-dipole interaction Hamiltonian between the two spins.

We will consider the spin operators $\vec{S}_1$ and $\vec{S}_2$ in the NV own basis : the z orientation of the S_z operator is chosen along the NV axis of each spin. In the presence of a longitudinal magnetic field, the sense of $\hat{z}$ will be chosen such that $\vec{B} \cdot \hat{z} > 0$, and the $\hat{x}$ direction is chosen along the transverse magnetic or electric field, whichever dominates the single spin Hamiltonian. These choices mean that there will be two distinct Cartesian basis $\{\hat{x}_1, \hat{y}_1, \hat{z}_1\}$ and $\{\hat{x}_2, \hat{y}_2, \hat{z}_2\}$ describing the two spins.

The dipole-dipole Hamiltonian can then be decomposed as :

$$-\frac{\mathcal{H}_{\text{dd}}}{J_0/r^3} = 3\left(\vec{S}_1 \cdot \hat{u}\right)\left(\vec{S}_2 \cdot \hat{u}\right) - \vec{S}_1 \cdot \vec{S}_2 \tag{7}$$

$$= \left[3(\hat{u} \cdot \hat{x}_1)(\hat{u} \cdot \hat{x}_2) - \hat{x}_1 \cdot \hat{x}_2\right] S_x^1 S_x^2 \tag{8}$$

$$+ \left[3(\hat{u} \cdot \hat{y}_1)(\hat{u} \cdot \hat{y}_2) - \hat{y}_1 \cdot \hat{y}_2\right] S_y^1 S_y^2 \tag{9}$$

$$+ \left[3(\hat{u} \cdot \hat{x}_1)(\hat{u} \cdot \hat{y}_2) - \hat{x}_1 \cdot \hat{y}_2\right] S_x^1 S_y^2 \tag{10}$$

$$+ \left[3(\hat{u} \cdot \hat{y}_1)(\hat{u} \cdot \hat{x}_2) - \hat{y}_1 \cdot \hat{x}_2\right] S_y^1 S_x^2 \tag{11}$$

$$+ \left[3(\hat{u} \cdot \hat{z}_1)(\hat{u} \cdot \hat{z}_2) - \hat{z}_1 \cdot \hat{z}_2\right] S_z^1 S_z^2 \tag{12}$$

$$+ \mathcal{H}_{\text{other}} \tag{13}$$

Where $J_0 = \frac{\mu_0 \gamma_e^2 \hbar^2}{4\pi} = (2\pi)52$ MHz $\cdot$ nm^3, $\vec{r} = r\vec{u}$ is the distance between the two spins and $\mathcal{H}_{\text{other}}$ contains terms of the form $S_{x/y}^i S_z^j$ which couple states far from resonance and will be neglected here.

C. Flip-flops in the magnetic basis $\{|0\rangle, |+1\rangle, |-1\rangle\}$

We will first consider the case, treated in [2], where the longitudinal magnetic field is strong enough that the single spin Hamiltonian eigenstates of both spins are close to

$\{|0\rangle, |+1\rangle, |-1\rangle\}$ (since we are interested in near-resonant spins, this means that both spins see roughly the same longitudinal and transverse magnetic field).

In this scenario, only flip-flop terms (that is $\langle \pm 1, 0|\mathcal{H}_{\mathrm{dd}}|0, \pm 1\rangle$) can couple two resonant two-spins states. Following the notation in [2], we introduce the dimensionless factor η defined as :

$$\eta^2 = \frac{1}{3}\left| \langle \pm 1, 0|\frac{\mathcal{H}_{\mathrm{dd}}}{J_0/r^3}|0, \pm 1\rangle \right|^2 \frac{4\gamma_f^2}{(\omega_f - \omega_{NV})^2 + 4\gamma_f^2} \tag{14}$$

Where γ_f is the fluctuator lifetime, ω_f the fluctuator angular frequency and ω_{NV} the NV angular frequency.

This numerical factor is linked to the previously mentioned $\bar{\eta}$ by averaging over every possible orientation and angular position of the fluctuators. Assuming that the fluctuators are evenly distributed among all four classes (NV axis orientation) and decomposing the $\vec{r}$ vector in the spherical basis (r, θ, ϕ), we can write $\bar{\eta}$ as :

$$\bar{\eta} = \frac{1}{4}\sum_{i=1}^{4}\int_\theta\int_\phi\int_{\omega_f}\int_{\omega_{NV}} |\eta(\vec{u}, i, \omega_{NV}, \omega_f)|\, d\Omega\, \rho(\omega_{NV})d\omega_{NV}\, \rho^i(\omega_f)d\omega_f \tag{15}$$

Where $d\Omega = \sin\theta d\theta d\phi$, $\rho(\omega_{NV})$ is the distribution of angular frequencies of the probed NV centers, and $\rho^i(\omega_f)$ is the distribution of angular frequencies for the fluctuators of class i.

While the distributions $\rho(\omega_{NV})$ and $\rho^i(\omega_f)$ can be approximated using the data presented in Fig. 6, we will assume that these distributions are independent of the external magnetic field, and since we are interested in comparing the same sample for various values of the magnetic field, we will simplify eq.(15) by postulating that $\frac{4\gamma_f^2}{(\omega_f - \omega_{NV})^2 + 4\gamma_f^2} = 1$ if the NV center's and the fluctuator's classes are resonant (or if they are from the same class), and $\frac{4\gamma_f^2}{(\omega_f - \omega_{NV})^2 + 4\gamma_f^2} = 0$ otherwise.

With these hypothesis, we found that there were 3 possible scenarios where the NV and fluctuator were resonant:

- The NV and fluctuator are resonant and from the same class (the angle $\widehat{z_1 z_2} = 0$) : this is always true, regardless of the magnetic field. We can analytically compute $\bar{\eta}$ in this case and find :

$$\bar{\eta}_{same} = \frac{1}{4}\int_\theta\int_\phi |\eta(\vec{u}, \widehat{z_1 z_2} = 0, \omega_{NV} = \omega_f)|\, d\Omega = \frac{1}{4}\cdot\sqrt{\frac{1}{3}}\cdot\frac{2}{3\sqrt{3}} \approx 5.55 \cdot 10^{-2}$$
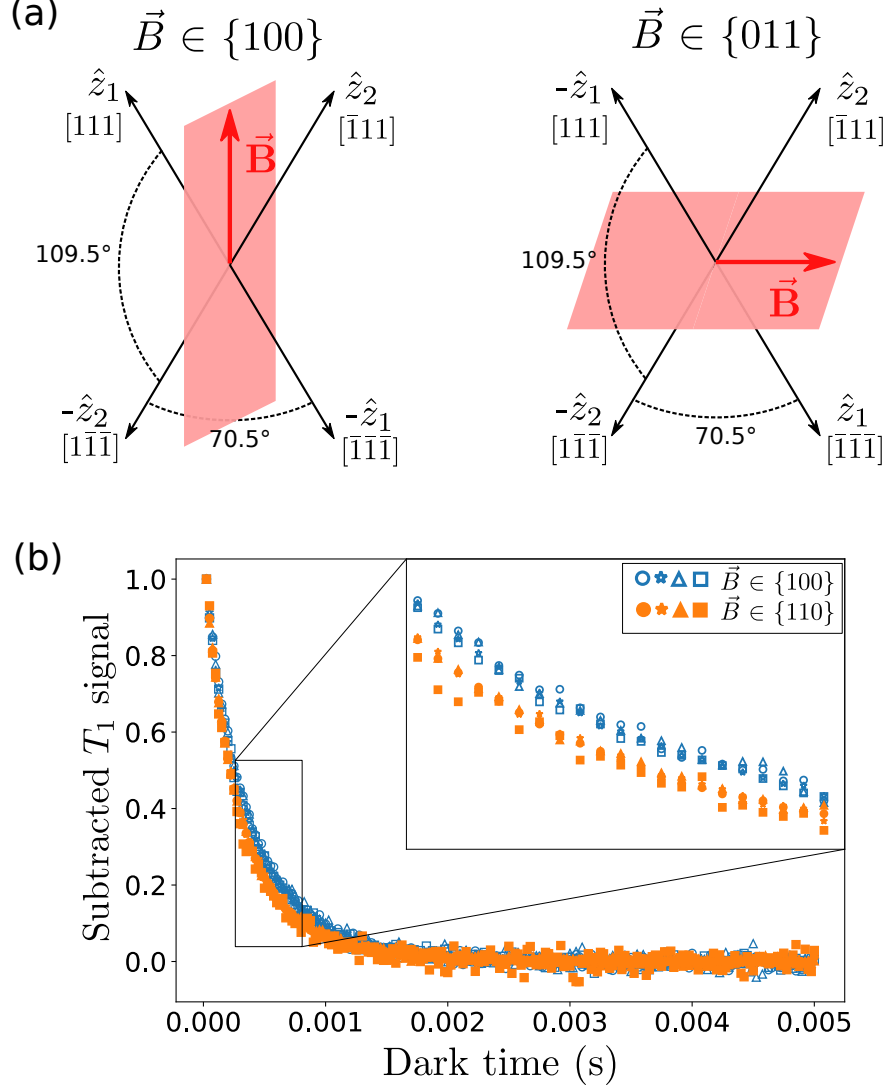
FIG. 9. (a) Geometrical representation of two NV classes and the two possible planes where the magnetic field has the same projection on both classes. The positive $\hat{z}_i$ direction is chosen so that $\vec{B} \cdot \hat{z}_i > 0$. (b) T_1 measurement on a two-class resonance following the protocol described in main text. 8 different magnetic field were used on the same sample : 4 times in a $\{100\}$ plane (blue unfilled symbols) and 4 times in a $\{110\}$ plane (orange filled symbols). Inset : zoom-in on the 0.3-0.8 ms region.

- The NV and fluctuator are resonant and the angle $\widehat{z_1 z_2} = \arccos(\frac{1}{3}) \approx 70.5°$. This happens when the magnetic field lies in the $\{100\}$ crystalline planes family. In this case we can numerically compute $\bar{\eta}_{\text{close}} \approx \frac{1}{4} \cdot \sqrt{\frac{1}{3}} \cdot 0.6507 \approx 9.39 \cdot 10^{-2}$

- The NV and fluctuator are resonant and the angle $\widehat{z_1 z_2} = \arccos(-\frac{1}{3}) \approx 109.5°$. This

happens when the magnetic field lies in the $\{110\}$ or $\{1\bar{1}0\}$ crystalline planes family. In this case we can numerically compute $\bar{\eta}_{\text{far}} \approx \frac{1}{4} \cdot \sqrt{\frac{1}{3}} \cdot 0.8328 \approx 1.20 \cdot 10^{-1}$. This last case was not taken into account by [2].

Fig. 9(a) shows a graphical representation of the difference between the two last scenarios : due to the $\vec{B} \cdot \hat{z} > 0$ condition, the same two classes of NV centers can have a $\widehat{z_1 z_2}$ angle equal to 70.5° or 109.5° depending on the external magnetic field.

These computed values can be tested experimentally. Fig. 9(b) shows the subtracted T_1 signal measured on the same sample [REF] for 8 different values of the magnetic field, each time on a two-class resonance : in 4 cases the magnetic field was in a $\{100\}$ plane, and in the 4 other cases it was in a $\{110\}$ plane. We can see that the measured lifetime is always smaller on the $\{110\}$ case, which corresponds the the greater $\bar{\eta}$ factor computed previously.

Here is a list of the computed values of $\bar{\eta}^2$, which according to eq.(4) is proportional to the dipole induced decay rate, for various magnetic field orientation. An ODMR spectrum for each of these situations is present in Fig. 10.

- Random orientation / no class degeneracy : for all four classes, $\bar{\eta} = \bar{\eta}_{\text{same}}$ and $\bar{\eta}^2 = 3.08 \cdot 10^{-3} \equiv \bar{\eta}_0^2$

- $\vec{B} \in \{110\}$: For the two non resonant classes : $\bar{\eta} = \bar{\eta}_{\text{same}}$ and $\bar{\eta}^2 = \bar{\eta}_0^2$. For the two resonant classes : $\bar{\eta} = \bar{\eta}_{\text{same}} + \bar{\eta}_{\text{far}}$ and $\bar{\eta}^2 \approx 10.0\bar{\eta}_0^2$

- $\vec{B} \in \{100\}$: For each pair of two-classes resonance: $\bar{\eta} = \bar{\eta}_{\text{same}} + \bar{\eta}_{\text{close}}$ and $\bar{\eta}^2 \approx 7.24\,\bar{\eta}_0^2$.

- $\vec{B} \parallel \langle 111 \rangle$: For the non-resonant class (parallel to $\vec{B}$) : $\bar{\eta} = \bar{\eta}_{same}$ and $\bar{\eta}^2 = \bar{\eta}_0^2$. For the triply resonant classes: $\bar{\eta} = \bar{\eta}_{\text{same}} + 2\bar{\eta}_{\text{far}}$ and $\bar{\eta}^2 \approx 28.4\,\bar{\eta}_0^2$.

- $\vec{B} \parallel \langle 100 \rangle$: For the quadruple resonance : $\bar{\eta} = \bar{\eta}_{\text{same}} + 2\bar{\eta}_{\text{close}} + \bar{\eta}_{\text{far}}$ and $\bar{\eta}^2 \approx 42.8\,\bar{\eta}_0^2$.

The measured increase in the decay rate is generally smaller than the predicted one : we measured an increase by a factor ~ 4 for a two-class degeneracy instead of the predicted 10.0, and an increase by a factor ~ 16 for a four-class degeneracy instead of the predicted 42.8. [2] measured an increase by a factor ~ 4 on a two-class degeneracy instead of the predicted 7.24 or 10.0.
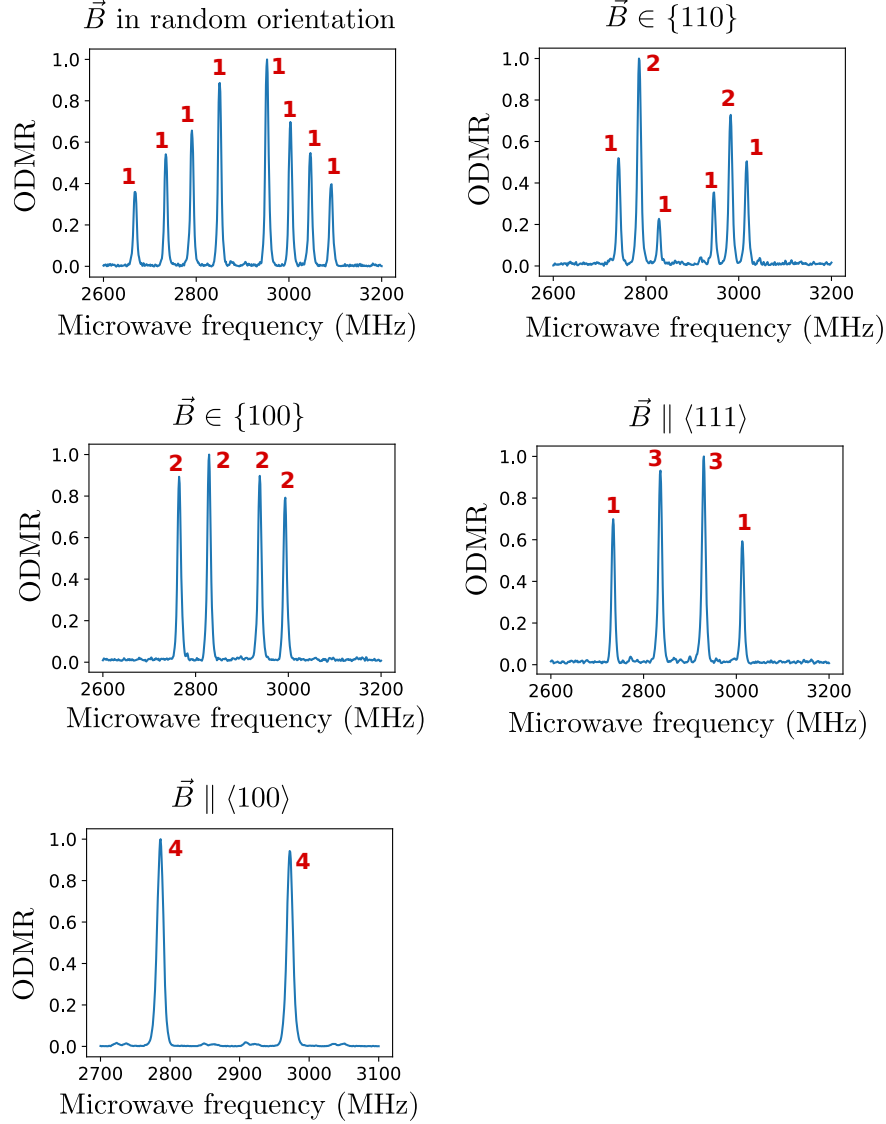
FIG. 10. ODMR spectra for different orientations of the magnetic field. Red numbers represent the number of degenerated classes for each line of the spectrum

D. Flip-flops in the non-magnetic basis $\{|0\rangle, |+\rangle, |-\rangle\}$

As described in sec. I, when the single spin Hamiltonian of the NV center is dominated by the electric field or the transverse magnetic field (as long as $\gamma_e B_\perp \ll D$), the eigenbasis of the NV Hamiltonian is close to $\{|0\rangle, |+\rangle = \frac{|+1\rangle + |-1\rangle}{\sqrt{2}}, |-\rangle = \frac{|+1\rangle - |-1\rangle}{\sqrt{2}}\}$. We therefore have to rewrite the dipole-dipole Hamiltonian using this new basis for both spins in order to perform similar calculations as the ones done in the previous section.

$\bar{\eta}$ table	$\widehat{z_1 z_2} = 0$	$\widehat{z_1 z_2} = 70.5°$	$\widehat{z_1 z_2} = 109.5°$
$|\pm 1\rangle$ basis	$\frac{2}{3\sqrt{3}} = 0.3849$	0.6507	0.8328
$|+/-\rangle$ basis $\hat{x}_1 \neq \hat{x}_2$	0.7110	0.6828	0.6828
$|+/-\rangle$ basis $\hat{x}_1 = \hat{x}_2$	$\frac{4}{3\sqrt{3}} = 0.7698$	0.6951	0.6951

TABLE I. Computation of $\dfrac{\bar{\eta}}{\frac{1}{4} \cdot \sqrt{\frac{1}{3}}}$ for the different eignebasis of the single spin Hamiltonian, and for the different angles between the z axis of the two spins.

Since the flip-flop processes are now of the form $|0, \pm\rangle \langle \pm, 0|$, we redefine the η factor as :

$$\eta^2 = \frac{1}{3} \left| \langle \pm, 0| \frac{\mathcal{H}_{\mathrm{dd}}}{J_0/r^3} |0, \pm\rangle \right|^2 \frac{4\gamma_f^2}{(\omega_f - \omega_{NV})^2 + 4\gamma_f^2} \tag{16}$$

In this new basis, the spin operators are written :

$$S_x = \begin{pmatrix} 0 & 1 & 0 \\ 1 & 0 & 0 \\ 0 & 0 & 0 \end{pmatrix} \begin{matrix} \langle -| \\ \langle 0|, \\ \langle +| \end{matrix} \quad S_y = \begin{pmatrix} 0 & 0 & 0 \\ 0 & 0 & 1 \\ 0 & 1 & 0 \end{pmatrix} \begin{matrix} \langle -| \\ \langle 0|, \\ \langle +| \end{matrix} \quad S_z = \begin{pmatrix} 0 & 0 & 1 \\ 0 & 0 & 0 \\ 1 & 0 & 0 \end{pmatrix} \begin{matrix} \langle -| \\ \langle 0| \\ \langle +| \end{matrix} \tag{17}$$

The symmetry in the (xy) plane is broken by the presence of the transverse electric or magnetic field. The x_i direction is defined as the direction of the transverse electric or magnetic field which dominates the single spin Hamiltonian of the particle i.

We will consider two cases :

- The x direction is defined by an external field (transverse magnetic field or strong external electric field) projected on the (xy) plane of each classes. In particular this means that two spins from the same class have the same $(\hat{x}, \hat{y}, \hat{z})$ basis.

- The x direction is defined by the local electric field generated by the charges in the crystal. We will assume that there are no correlations in the electric field between the NV and fluctuator, and will sample a random angle $\psi \in [0, 2\pi]$ between the axes $\hat{x}_1$ and $\hat{x}_2$.

For this two cases, which we will call $\hat{x}_1 = \hat{x}_2$ and $\hat{x}_1 \neq \hat{x}_2$, we can compute the $\bar{\eta}$ factor for the three scenarios discussed previously : $\widehat{z_1 z_2} = 0$ (same class), $\widehat{z_1 z_2} = 70.5°$ and $\widehat{z_1 z_2} = 109.5°$. The results, as well as those in the $|\pm 1\rangle$ basis are presented in Table I.

There are two particular situations where these values can be experimentally tested :

The first one is described in Fig. [REF] of the main text : in the presence of pure transverse magnetic field (for a single class, non-resonant with the three other classes), the decay rate of the class decreases with the magnetic field amplitude, due to the double-flip processes (described below), and then reaches a plateau with a decay rate value ~ 2 times bigger than in the longitudinal magnetic field case. This increase is in agreement with the fact that $\bar{\eta}_{\text{same}}$ is 2 times bigger in the non-magnetic $|+/-\rangle$ basis than in the magnetic $|\pm 1\rangle$ basis. The measured increase is again smaller than the predicted factor of 4 given by eq. (4).

The second one is the difference between the $\vec{B} \parallel \langle 100 \rangle$ case and the $\vec{B} = 0$ case. When a magnetic field is applied in the [100] direction, all four classes are resonant and the spin Hamiltonian basis is $\{|0\rangle, |+1\rangle, |-1\rangle\}$. The $\bar{\eta}$ factor in this case has been calculated in the previous section : $\bar{\eta}^2 \approx 42.8 \, \bar{\eta}_0^2$. When no external magnetic field is applied, all four classes are also resonant but the spin Hamiltonian basis is $\{|0\rangle, |+\rangle, |-\rangle\}$ (see Sec. 1) and double-flip processes are near-resonant. The decay rate due purely to flip-flop in the $|+/-\rangle$ basis is proportional to $\bar{\eta}^2 = (\bar{\eta}_{\text{same}}^{+/-} + 3\bar{\eta}_{\text{diff}}^{+/-})^2 \approx 51.4 \, \bar{\eta}_0^2$. Fig. [REF] of the main text shows that we indeed observe a shorter lifetime when $\vec{B} = 0$, in agreement with the higher value of $\bar{\eta}^2$, but this decrease could also come from the double-flip processes which are absent when $\vec{B} \neq 0$.

E.   Double-flip processes

Double-flip processes, that is processes where the two spins flip in the same direction, compared to flip-flop where the two spins flip in opposite directions, are related to matrix elements such as $\langle +1, 0| \frac{\mathcal{H}_{\text{dd}}}{J_0/r^3} |0, -1\rangle$ in the $|\pm 1\rangle$ basis or $\langle +, 0| \frac{\mathcal{H}_{\text{dd}}}{J_0/r^3} |0, -\rangle$ in the $|\pm\rangle$ basis. These matrix elements couple two-spin states that are never fully resonant, however with low-to zero magnetic, the residual splitting due to local electric and magnetic field (~ 6 MHz with our samples) is small enough compared to the fluctuators linewidth measured in sec. IV B to be ~ 8 MHz, so that double-flip processes may still occur.

Fig. [REF] of the main text shows that for lower transverse field values, the spin decay rate is increased significantly. We attribute this increase to double-flip processes. We can see that the decay rate increase (~ 5 times the baseline value) is significantly higher than the increase due solely to the $|+/-\rangle$ basis (~ 2 times the baseline value). This lead us to believe that the double-flip process are the main reason behind the decrease in spin lifetime for

$\vec{B} = 0$ observed in Fig. [REF] of the main text. This would probably mean that double-flip processes are the dominant factor in the sensitivity of the magnetometry protocol presented in the main text.

---

[1] SV Anishchik, VG Vins, AP Yelisseyev, NN Lukzen, NL Lavrik, and VA Bagryansky. Low-field feature in the magnetic spectra of nv- centers in diamond. *New Journal of Physics*, 17(2):023040, 2015.

[2] Joonhee Choi, Soonwon Choi, Georg Kucsko, Peter C. Maurer, Brendan J. Shields, Hitoshi Sumiya, Shinobu Onoda, Junichi Isoya, Eugene Demler, Fedor Jelezko, Norman Y. Yao, and Mikhail D. Lukin. Depolarization Dynamics in a Strongly Interacting Solid-State Spin Ensemble. *Phys. Rev. Lett.*, 118(9):093601, March 2017. Number: 9.

[3] DS Filimonenko, VM Yasinskii, AP Nizovtsev, S Ya Kilin, and Fedor Jelezko. Weak magnetic field effects on the photoluminescence of an ensemble of nv centers in diamond: experiment and modelling. *Semiconductors*, 54(12):1730–1733, 2020.

[4] Thomas Mittiga, Satcher Hsieh, Chong Zu, Bryce Kobrin, Francisco Machado, Prabudhya Bhattacharyya, NZ Rui, Andrey Jarmola, Soonwon Choi, Dmitry Budker, et al. Imaging the local charge environment of nitrogen-vacancy centers in diamond. *Physical review letters*, 121(24):246402, 2018.

[5] Eric Van Oort and Max Glasbeek. Electric-field-induced modulation of spin echoes of nv centers in diamond. *Chemical Physics Letters*, 168(6):529–532, 1990.